Biogeosciences Discuss., 10, 1177–1205, 2013
www.biogeosciences-discuss.net/10/1177/2013/
doi:10.5194/bgd-10-1177-2013

Biogeosciences Discussions

Nested atmospheric inversion for the terrestrial carbon sources and sinks in China

F. Jiang[1,2], H. Wang[1,2], J. M. Chen[1,2,4], W. Ju[1,2], and A. Ding[3]

[1]Jiangsu Provincial Key Laboratory of Geographic Information Science and Technology, Nanjing University, Nanjing, China
[2]International Institute for Earth System Science, Nanjing University, Nanjing, China
[3]School of Atmospheric Sciences, Nanjing University, Nanjing, China
[4]Department of Geography and Program in Planning, University of Toronto, Toronto, Canada

Received: 15 December 2012 – Accepted: 28 December 2012 – Published: 25 January 2013

Correspondence to: F. Jiang (jiangf@nju.edu.cn)

Published by Copernicus Publications on behalf of the European Geosciences Union.

Abstract

In this study, we establish a nested atmospheric inversion system with a focus on China using the Bayes theory. The global surface is separated into 43 regions based on the 22 TransCom large regions, with 13 small regions in China. Monthly CO_2 concentrations from 130 GlobalView sites and a Hong Kong site are used in this system. The core component of this system is atmospheric transport matrix, which is created using the TM5 model with a horizontal resolution of $3^\circ \times 2^\circ$. The net carbon fluxes over the 43 global land and ocean regions are inverted for the period from 2002 to 2009. The inverted global terrestrial carbon sinks mainly occur in Boreal Asia, South and Southeast Asia, eastern US and southern South America (SA). Most China areas appear to be carbon sinks, with strongest carbon sinks located in Northeast China. From 2002 to 2009, the global terrestrial carbon sink has an increasing trend, with the lowest carbon sink in 2002. The inter-annual variation (IAV) of the land sinks shows remarkable correlation with the El Niño Southern Oscillation (ENSO). However, no obvious trend is found for the terrestrial carbon sinks in China. The IAVs of carbon sinks in China show strong relationship with drought and temperature. The mean global and China terrestrial carbon sinks over the period 2002–2009 are -3.15 ± 1.48 and $-0.21 \pm 0.23\,\mathrm{Pg\,C\,yr^{-1}}$, respectively. The uncertainties in the posterior carbon flux of China are still very large, mostly due to the lack of CO_2 measurement data in China.

1 Introduction

Carbon dioxide (CO_2) and other greenhouse gas emitted from human activities are the main cause of global warming (IPCC, 2007). In 2009, the carbon emissions from fossil fuel combustion, cement production and land use change reached $10\,\mathrm{Pg\,C\,yr^{1}}$ (Le Quéré et al., 2009), about 55 % of these CO_2 were detained in the atmosphere (IPCC, 2007), leading to the increase in atmospheric CO_2 concentration at an unprecedented rate (about $1.8\,\mathrm{ppm\,yr^{-1}}$). At the present, China has become the largest CO_2 emitter in

BGD
10, 1177–1205, 2013

Title Page
Abstract | Introduction
Conclusions | References
Tables | Figures
◀| |▶
◀ ▶
Back | Close
Full Screen / Esc
Printer-friendly Version
Interactive Discussion

the world, and will continue to increase in the near future due to with population growth and economic development.

Terrestrial ecosystems play a very important role on regulating the atmospheric CO_2 concentration. In 1990s and during 2000–2005, on average, terrestrial ecosystems absorbed 1.0 ± 0.6 and $0.9 \pm 0.6\,PgC\,yr^{-1}$ carbon from the atmosphere, accounting for about 16 % and 13 % of the emissions from fossil fuel combustion and cement production, respectively (IPCC, 2007). During 1980–2000, the carbon sinks of forests, grasslands, and shrubs in China were 0.075, 0.007, and −0.014– −0.024 $PgC\,yr^{-1}$, respectively, which in total offset 20.0–26.8 % of the China's industrial carbon emissions (Fang et al., 2007). Based on the 1999–2003 national forest inventory, Wang et al. (2010) calculated the carbon sink of China's forest was $-0.21\,PgC\,yr^{-1}$, while using the InTEC model, Wang et al. (2007) simulated the forest carbon sink to be $0.18 \pm 0.05\,PgC\,yr^{-1}$ during 1988–2001. Cao et al. (2003) studied the spatial distribution characteristics of ecosystem carbon sinks and its response to climate change and elevated atmospheric CO_2 concentration using the CEVSA model, their results showed that, in the past 20 yr, China was a weak carbon sink, but, arid and warming climate in the future may turn it into a carbon source. However, since it is very difficult to obtain detail inventories of soil carbon storage and forest resources, the carbon sink estimation based on inventories still have large uncertainties. Simulations using ecosystem models are highly dependent on model structure, model parameters and input data, and there also have large uncertainties.

Atmospheric inversion is a method, which uses the measurements of atmospheric CO_2 concentrations to optimize land and ocean carbon fluxes. Its main idea is that the CO_2 concentrations at one site can be affected by the surface carbon fluxes through atmosphere transport under the assumption that the calculation errors of atmospheric transport are much smaller than the errors in estimating surface carbon fluxes, then, the errors of surface carbon fluxes could be corrected according to the biases between observations and simulations of the concentration. With this method, many studies have been conducted to estimate the global terrestrial carbon fluxes (e.g. Denning et al.,

BGD
10, 1177–1205, 2013

1999; Ciais, et al., 2000; Gurney et al., 2002; Law et al., 2003). However, these studies were generally conducted with low spatial and temporal resolutions. For example, TransCom only separated global surface into 11 land areas and 11 marine areas, and inverted at monthly time step (Gurney et al., 2002). In order to improve the resolution of the particular region, several regional inversion techniques have been developed (e.g. Gerbig et al., 2003; Peylin et al., 2005; Schuh et al., 2010). Deng et al. (2007) developed a nested atmospheric inversion method, in which the central region is divided into a number of cells, while large regions remain the same outside of the central region. This method can reduce the uncertainty caused by setting boundary conditions for the central region of the main interest. Based on this method, Deng et al. (2007) successfully inverted carbon sources and sinks for North America in a relatively high resolution (30 small regions). In this paper, based on the nested method we established a China-focused nested atmospheric inversion system. Using this system, we investigate the spatial distribution of terrestrial ecosystems carbon sources and sinks in China as well as their interannual variations during 2002–2009. The description of the inversion system is presented in Sect. 2, and the inverted spatial pattern of terrestrial carbon fluxes as well as their inter-annual variations are presented and discussed in Sect. 3.

2 Nested inversion system

The observed CO_2 concentration at one time and one place is contributed by the transport of the fluxes from all global regions for a past period of time and the initial well-mixed CO_2 concentration. The transport contributions could be expressed as a transport operator multiplied by the fluxes. So, if we have enough CO_2 observations, the transport operator and the initial CO_2 concentration, the fluxes could be known. In this study, we use the time-dependent Bayesian synthesis method to solve this inversion problem. Details about this method could be found in Deng et al. (2007). The key of this method is to reduce to minimizing the following cost function (Enting et al., 1995;

Rayner et al., 1999).

$$J = \frac{1}{2}(\mathbf{M}s - \mathbf{c})^{\mathrm{T}} R^{-1} (\mathbf{M}s - \mathbf{c}) + \frac{1}{2}(s - s_{\mathrm{p}})^{\mathrm{T}} Q^{-1} (s - s_{\mathrm{p}}) \quad (1)$$

where **M** is a matrix representing the transport operator; **c** is the observations; ***s*** is the unknown vector of the carbon flux of all regions at different times combined with the initial well-mixed atmospheric CO_2 concentration; s_{p} is a priori estimation of ***s***; and R and Q are the uncertainties of **c** and s_{p}, respectively. By minimizing this cost function, the posterior fluxes ***s*** could be obtained as:

$$\hat{s} = (\mathbf{M}^{\mathrm{T}} R^{-1} \mathbf{M} + Q^{-1})^{-1} (\mathbf{M}^{\mathrm{T}} R^{-1} \mathbf{c} + Q^{-1} s_{\mathrm{p}}) \quad (2)$$

2.1 Inversion regions

In this study, the global surface is separated into 43 regions based on the 22 TransCom large regions (e.g. Gurney et al., 2003; Baker et al., 2006), with 13 small regions in China (Fig. 1). The partition scheme in China is mainly based on land cover types, i.e. forest, crop, grass, and desert. Data of land cover is obtained from http://lpdaac.usgs.gov (LP DAAC, 2001). The forest in China is separated into 5 regions, i.e. South China (region 29), Southwest China (region 30), East China (region 31), center China (region 32), and Northeast China (region 33); the crop is separated into 4 regions, i.e. Sichuan Basin (region 37), North China crop region (mainly North China plain, region 38), Yangtze Plain (region 39) and Northeast China Plain (region 40); and the grass is partitioned into 3 regions, i.e. North China grass region (region 34), Southwest China grass region (region 35) and Northwest China grass region (region 36). The rest of Asia is separated into 8 regions They are Southeast Asia, indo-China peninsula, Indian peninsula, Japan, Korean peninsula, Mongolia, West Asia, and Boreal Asia. Temperate North America is separated into 2 regions due to the significant land cover difference between east and west temperate North America. In addition, Africa is partitioned into 3 regions in this study, i.e. North Africa, Tropical Africa, and South Africa (see Fig. 1).

BGD
10, 1177–1205, 2013

2.2 Transport modeling

Monthly transport operator **M** of ten years (January 2000 to December 2009) for the 43 regions are calculated using the global two-way nested transport model TM5 (Krol et al., 2005), which has been widely used in global atmospheric chemistry studies (e.g. Houweling et al., 1998; Dentener et al., 2003; Peters et al., 2002) and atmospheric inversion researches (e.g. Meirink et al., 2008; Krol et al., 2008; Deng and Chen, 2011). TM5 is an off-line model, which is driven by meteorological fields from the ECMWF model. In this study, TM5 is run at a horizontal resolution of $3^{\circ} \times 2^{\circ}$with 25 vertical layers with the top layer at about 1 hpa. Firstly, TM5 is modified to tag the CO_2 concentrations contributed from the carbon fluxes of each region. Then, the contributions of each month and each region to the CO_2 concentrations at each observation are calculated. In total, TM5 is run for 120 times, and each time, the model is continuously run for three years, with 1 Pg carbon emitted from each region in the first month, and no emissions in the subsequent months. The distribution of the 1 Pg carbon emissions in each terrestrial region is according to the annual mean NPP pattern, which is calculated using the BEPS model (Chen et al., 1999); while no distribution was considered for the ocean region. However, we assume that there is no carbon exchanges happen when the sea surface is covered by ice. Monthly sea ice data from the HadISST dataset (Rayner et al., 2003) is used in this study.

TM5 is also used in forward transport simulation from January 2000 to December 2009 for two types of fluxes in the same grid system with transport operator calculations. These two types of fluxes are (i) the fossil fuel emission field, which is obtained from Carbon Tracker 2010 (http://carbontracker.noaa.gov); and (ii) the monthly mean fire emission available from the Global Emissions Fire Database version 3 (GFEDv3) (van der Werf et al., 2010). As we assume that these two fluxes have been correctly estimated, the CO_2 concentrations from the contributions of these fluxes will be pre-subtracted in the inversion system. Hence, the matrix **c** in Eq. (1) can be further

BGD
10, 1177–1205, 2013

expressed as

$$\mathbf{c} = \mathbf{c}_{obs} - \mathbf{c}_{ff} - \mathbf{c}_{fire} \quad (3)$$

where $\mathbf{c}_{obs}$ is the observed monthly CO_2 concentration; $\mathbf{c}_{ff}$ and $\mathbf{c}_{fire}$ are simulated ones by the forward simulation from fluxes (i) and (ii), respectively.

2.3 Priori fluxes and their uncertainties

Hourly terrestrial ecosystem carbon exchanges and daily carbon fluxes across the air-water interface are considered as priori fluxes. The former is simulated using the BEPS model, which is a process-based, remote sensing data driven, and mechanical ecosystem model (Chen et al., 1999; Ju et al., 2006). The annual fluxes at each grid are neutralized according to the work of Deng and Chen (2011). The latter is modeled using the OPA-PISCES-T model, which is a state-of-the-art combined global ocean circulation (OPA) and biogeochemistry model (PISCES-T) (Buitenhuis et al., 2006).

There are many sources of uncertainty in the model simulation, including errors in the meteorological data, errors of model parameters, and errors caused by the model structure. So, estimating the uncertainties of the simulated carbon fluxes is extremely difficult. In this study, we use an uncertainty of 2.0 $PgC\,yr^{-1}$ for the global land surface (Deng and Chen, 2011), and an uncertainty of 0.67 $PgC\,yr^{-1}$ for the global ocean surface (Baker et al., 2006). The uncertainty on the land is spatially distributed based on the annual NPP distribution simulated by BEPS, while the one on the ocean is distributed according to the area of each ocean region. These prior uncertainties are also in the range of those used in previous studies (e.g. Rödenbeck et al., 2003; Gurney et al., 2004; Bruhwiler et al., 2007).

2.4 Observations and model-data mismatch errors

CO_2 observations from 131 sites are used in this study, in which 130 time series are from GLOBALVIEW-CO_2 2010 dataset, including 54 flask observations, 7 continuous measurements, 5 tower sites, 6 ship sites, and 58 aircraft sites (aircraft at each flight level is considered as 1 site), and 1 site (i.e. HKO) is obtained from the website of the World Data Centre for Greenhouse Gas (http://ds.data.jma.go.jp/gmd/wdcgg/). There are over 300 time series of observations in GLOBALVIEW-CO_2 2010 dataset, which were derived by many different organizations. The dataset is a product of the observations, including smoothed values, and interpolated and extrapolated values. In this study, we select data according to the following principle: (1) only smoothed values are selected; (2) if there are many stations in one region, only the data from NOAA Earth System Research Laboratory (ESRL) are selected (e.g. North America), while if only few stations in one region, the data from other organizations are also considered (e.g. Asia); (3) we generally do not choose tower observations unless there are very few observations in that area. And if one tower station is selected, only the top-level observations are used; and (4) usually, the stations near large city or airport are not used. The locations of the sites are shown in Fig. 1.

The estimation of the model-data mismatch errors is very difficult (Bruhwiler et al., 2007), since the errors come from both the observations (instrument errors) and the simulations. Various methods (e.g. Rayner et al., 1999; Gurney et al., 2004; Michalak et al., 2005) have been used to determine the model-data mismatch errors. In this study, the data-mismatch error is defined using the following function, which is similar to Peters et al. (2005) and Deng and Chen (2011).

$$R = \sigma_{\text{const}}^2 + \text{GVsd}^2 \tag{4}$$

where GVsd reflects the observation error, which is the standard deviation of the residual distribution in the average monthly variability (var) file of GLOBALVIEW-CO_2 2010, and the constant portion σ_{const} reflects the simulation error, due to the different performances of the model on each observation station. This portion also varies with station. Except for some difficult stations, the observation sites are divided into 5 categories. The categories and respective value are: Antarctic sites/oceanic flask and continuous sites (0.30), ship and tower sites (1.0), mountain sites (1.5), aircraft samples (0.5), and

Discussion Paper | Discussion Paper | Discussion Paper | Discussion Paper |

BGD

10, 1177–1205, 2013

Nested Inversion for carbon sinks in China

F. Jiang et al.

land flask/continuous sites (0.75). The value of 3.5 is used for the difficult sites (e.g. abp_01D0, bkt_01D0).

3 Results and discussion

3.1 Inverted global carbon fluxes

Figure 2 shows the inverted mean distribution of terrestrial and ocean carbon fluxes for 2002–2009. Most of the land regions are inverted as carbon sinks, with strong sinks occurring in Boreal Asia, South and Southeast Asia, eastern US and Southern South America (SA), while Tropical America and Southern Africa release carbon to the atmosphere. This spatial pattern is quite consistent with the MODIS global NPP changes from 2000 through 2009 (Zhao and Running, 2010), especially in Africa, North America and Eurasia. However, the flux pattern in southern SA and Southeast Asia are inconsistent with the changes in MODIS NPP, indicate that there may be large uncertainties existed in these regions. The estimated global terrestrial ecosystem carbon sink is $-3.15 \pm 1.48\,\mathrm{Pg\,C\,yr^{-1}}$ (Table 1), which is slightly lower than the result of Deng and Chen (2011) ($-3.63 \pm 0.49\,\mathrm{Pg\,C\,yr^{-1}}$), who did global carbon inversion from 2002 to 2007, and close to the land sink estimated by Le Quéré et al. (2009) (2000–2008, $-3.0 \pm 0.9\,\mathrm{Pg\,C\,yr^{-1}}$) using five global vegetation models.

Figure 3 shows the interannual variation (IAV) of the inverted global land carbon sinks. For comparison, the IAVs from Deng and Chen (2011) and Le Quéré et al. (2009) are also shown. The global IAV of land sinks is $3.16\,\mathrm{Pg\,C\,yr^{-1}}$, with range from $-1.35\,\mathrm{Pg\,C\,yr^{-1}}$ to $-4.51\,\mathrm{Pg\,C\,yr^{-1}}$. From 2002 to 2009, the global terrestrial carbon sink has an increasing trend. It increases from 2002 to 2004, and decreases in 2005, then continuing to increase until 2008, and decrease in 2009. There is lowest land carbon sink in 2002 ($-1.35\,\mathrm{Pg\,C\,yr^{-1}}$), and highest land sink in 2008 ($-4.51\,\mathrm{Pg\,C\,yr^{-1}}$). The IAV of the land sinks shows remarkable correlation with the El Niño Southern Oscillation (ENSO), the weaker land sinks in 2002, 2005 and 2009

BGD
10, 1177–1205, 2013

correspond to the strong El Niño events happened in 2002–03, 2004–05 and 2009–10 respectively, while the stronger land sink in 2008 corresponds to the La Niña event (http://www.esrl.noaa.gov/psd/enso/mei/). The mechanism of the impact of ENSO on terrestrial carbon sinks has been studied by Zeng et al. (2005). In this study, the IAVs are dominated by the tropical land fluxes. Gurney et al. (2012) quantitatively investigated the relationship between ENSO and tropical net carbon exchange, and showed that the warm phase of ENSO (El Niño events) could explain more than 70 % of the variability in tropical net carbon exchange.

The increasing trend in the terrestrial sink in this study agrees well with Deng and Chen (2011) and Le Quéré et al. (2009). During 2002 to 2005, our results are in the range of Le Quéré et al. (2009) and Deng and Chen (2011), i.e. stronger than Le Quéré et al. (2009), but weaker than Deng and Chen (2011), while after 2006, the land sinks are lower than Le Quéré et al. (2009) and Deng and Chen (2011). The differences between this study and Le Quéré et al. (2009) may be partly attributed to different estimation on the fluxes induced by land use change (including fire emissions), while the ones between this study and Deng and Chen (2011) may due to the different inversion setups, e.g. selection in observations, estimations in model-data mismatch errors, and so on. Overall, these results indicate that the terrestrial carbon fluxes inverted in this study are quite reasonable.

3.2 Inverted China carbon fluxes

As shown in Fig. 2, most China areas appear to be carbon sinks, with strongest carbon sinks locate in Northeast China ($> 50\,\mathrm{g\,C\,m^{-2}\,yr^{-1}}$). Large carbon sinks ($> 30\,\mathrm{g\,C\,m^{-2}\,yr^{-1}}$) also occur in the North China crop region, Southeast China forest region and Southwest China grass region. During 2002–2009, the inverted mean carbon sink in China is $-0.21 \pm 0.23\,\mathrm{Pg\,C\,yr^{-1}}$, in which 34 % are absorbed in Northeast China (including regions 33 and 40), 25 % are captured in Southwest China (including regions 30, 35 and 37), and 18 % are contributed by Central and Eastern China region (including regions 31, 32, and 39). Basically, this spatial pattern agrees well

BGD
10, 1177–1205, 2013

with the NPP changes derived by Zhao and Running (2010). The inverted carbon sinks in this study is close to the result of Carbon Tracker (Peters et al., 2007) in 2010 ($0.25\,PgC\,yr^{-1}$) for the same period, but lower than the inversion ensemble result ($0.35 \pm 0.33\,PgC\,yr^{-1}$) over the period of 1996–2005, which is derived by Piao et al. (2009). When distinguishing different ecosystem regions, the forest, grass, and crop regions capture carbon of $-0.08\,PgC\,yr^{-1}$ (38 %), $-0.07\,PgC\,yr^{-1}$ (33 %) and $-0.06\,PgC\,yr^{-1}$ (29 %), respectively, which are also comparable with Carbon Tracker results.

Terrestrial ecosystems also emit carbon in the form of volatile organic compounds (BVOCs), and most of these BVOCs are oxidized to CO_2 in the atmosphere (Naik et al., 2004). Guenther (2002) noted that the predicted annual global reactive BVOC emissions of about 1.2 PgC could result in the annual production of approximately 1.0 PgC as CO_2 per year (83 %). Granier et al. (2000) estimated that about 80 % of the reactive the dominant BVOC (i.e. isoprene) got oxidized to CO_2. Hence, BVOCs play an important role in the global carbon budget and cycling. Most reactive BVOCs have short lifetime in the atmosphere (< 1 day). Therefore, the measured CO_2 concentrations have included the contributions from the oxidization of BVOCs. In addition, the inverted terrestrial carbon sinks in China also include the contributions from the consumptions of wood and food, which are imported from outside of China. Hence, when comparing the inversion results in this study with the results from ecosystem models or inventory based methods, then, these two contributions should be considered. In China, the emissions of reactive BVOCs (i.e. isoprene and monoterpene) are about $24\,TgC\,yr^{-1}$ (Jiang et al., 2012), which may contribute the CO_2 budget in the atmosphere about $0.019\,PgC\,yr^{-1}$. Based on Food and Agriculture Organization of the United Nations (FAO) statistical databases, Piao et al., (2009) estimated that 0.008 PgC of wood, and 0.004 PgC of food were imported into China every year. Hence, we estimate that China terrestrial ecosystem carbon sink is about $0.241\,PgC\,yr^{-1}$. This result is comparable with the result of Tian et al. (2011) ($-0.21 \pm 0.078\,PgC\,yr^{-1}$), who simulated the net exchanges of CO_2 between China's terrestrial ecosystems and the atmosphere during 1961–2005 using a highly integrated process-based ecosystem model (DLEM). Moreover, our result is slight higher than the values derived by Piao et al. (2009) using inventory-based ($-0.18 \pm 0.073\,\mathrm{Pg\,C\,yr^{-1}}$) and process-based model ($-0.17 \pm 0.073\,\mathrm{Pg\,C\,yr^{-1}}$) for the period of 1980s and 1990s, these probably imply the increase of the carbon sink in China in 2000s.

Since most reactive BVOCs are emitted from forest area (Jiang et al., 2012), while most imported food and wood are probably consumed in crop region. Therefore, we estimate that the carbon sinks of forest, grass, and crop region are −0.1, −0.07, and $-0.072\,\mathrm{Pg\,C\,yr^{-1}}$, respectively. Compared with previous studies, the carbon sink of forest land is comparable with the values of Tian et al., (2011), Piao et al. (2009) and Pan et al., (2011), while the carbon sinks of grassland and cropland are slight stronger than Tian et al. (2011) and Piao et al. (2009)'s results, the reason may be attributed to the fact that the grass and crop regions in this study include some forest covers. If we consider the contribution of the forest in grass and crop regions, the forest carbon sinks estimated in this study would be larger than the results of previous studies. Nevertheless, the estimation of the carbon sinks from different ecosystems are very rough, in order to derive more accurate carbon sinks for different ecosystems, more detailed regional partition schemes are needed.

Figure 4 shows the IAVs of the terrestrial ecosystem carbon sinks, fossil fuel carbon emissions, and net carbon fluxes in China. The IAV of carbon sinks in China is $0.24\,\mathrm{Pg\,C\,yr^{-1}}$, with range from $-0.11\,\mathrm{Pg\,C\,yr^{-1}}$ to $-0.35\,\mathrm{Pg\,C\,yr^{-1}}$. From 2002 to 2005, the carbon sink decreases year by year, and then increases in 2006, after that, it decreases again until 2008. The carbon sink is lowest in 2008. ($-0.11\,\mathrm{Pg\,C\,yr^{-1}}$), and highest in 2009 ($-0.35\,\mathrm{Pg\,C\,yr^{-1}}$). Overall, there is no obvious trend for the carbon sinks in China. These IAVs in China are not same as those for the globe. The main reason may be that the IAVs of global carbon sinks are dominated by the tropical land fluxes, which are highly affected by ENSO (Sect. 3.1), but the impacts of ENSO on tropical zone and on China may be different.

BGD
10, 1177–1205, 2013

Figure 5 shows the relationship between terrestrial carbon sinks and drought areas in China. The drought data during 2002 to 2008 are obtained from Zou et al. (2010). Obviously, there is a fairly strong relationship between the IAVs of carbon sinks and drought areas in China. From 2002 to 2005, the drought area has an increasing trend, corresponding to the decrease in carbon sinks. During 2004–2007, the droughts are relatively severe in China, with drought area maintaining more than 27 %, corresponding to relatively weaker carbon sinks in these years. However, there still exist some exceptional years, i.e. 2006 and 2008 which do not conform to this relationship. In 2006, the drought area is larger than previous two years, while the carbon sinks increased from 2005. On the contrary, the drought area is smallest in 2008, but the carbon sink is lowest in 2008 Inspecting the spatial pattern for the anomaly of the carbon sinks, we found that in 2006, the carbon sinks increased in all China terrestrial areas except in Northeast China, while in 2008, they decreased in most China except northern China (Fig. 6). Though there is relatively severe drought, the mean temperature is also higher than normal years in most China except in Northeast China in 2006 (Fig. 6a). Conversely, the mean temperature in 2008 is lower than normal years in most China except in northern China. These indicate that the IAVs of terrestrial carbon sinks may be influenced by air temperature as well in the meantime. Warming climate may lengthen the growing seasons, which may lead to much stronger carbon sinks. Figure 7 shows the IAVs of the annual mean temperature and the terrestrial carbon sink in China during 2002–2009, which clearly shows that from 2002 to 2005, the temperature has a decreasing trend, corresponding to the decrease of the carbon sinks, and the temperature increases in 2006 also corresponds to the increase of the carbon sink in 2006. The same correspondence is also found in 2008. Nevertheless, this correspondence does not exist in 2007 and 2009, indicating that the inverted IAVs in this study may still have large uncertainties. One of the reasons may be the shortage of the observation data, and the data within and around China used in this study do not reflect the situation of the whole China. Another reason may be attributed to the estimation of fossil fuel emissions, as economic crisis happened in the world since 2008.

BGD
10, 1177–1205, 2013

4 Summary and conclusions

A nested atmospheric inversion system with focus on China using the Bayes theory is established in this study. The global surface is separated into 43 regions based on the 22 TransCom large regions, with 13 small regions in China. Monthly CO_2 concentrations from 130 GlobalView sites and a Hong Kong site are used in this system. The TM5 model is used for calculating the monthly transport matrix, which is run in a horizontal resolution of $3^\circ \times 2^\circ$. The carbon fluxes of terrestrial ecosystems and the air-water interface are considered as priori fluxes, which are simulated using the BESP model and the OPA- PISCES-T model respectively.

Using this inversion system, we investigate the spatial and temporal characteristics of the global and China terrestrial ecosystem carbon fluxes during 2002–2009. The inverted global terrestrial carbon sinks mainly occur in Boreal Asia, South and Southeast Asia, eastern US and southern South America. Most China areas appear to be carbon sinks, with strongest carbon sinks locating in Northeast China. From 2002 to 2009, the global terrestrial carbon sink has an increasing trend, with the lowest carbon sink in 2002. However, no obvious trend was found over China's landmass. The inter-annual variations (IAVs) of the global land sinks show remarkable correlation with the El Niño Southern Oscillation (ENSO), while the IAVs in China show strong relationship with drought and temperature. The mean global and China terrestrial carbon sinks over the period 2002–2009 are -3.15 ± 1.48 and $-0.21 \pm 0.23\,\mathrm{Pg\,C\,yr^{-1}}$, respectively. Considering the emissions of biogenic volatile organic compounds (BVOCs) ($0.019\,\mathrm{Pg\,C\,yr^{-1}}$) and the import of wood and food ($0.012\,\mathrm{Pg\,C\,yr^{-1}}$), we estimate that the China terrestrial ecosystem carbon sink is about $-0.241\,\mathrm{Pg\,C\,yr^{-1}}$ during 2002–2009 which is comparable with previous studies.

Though large uncertainties still exist in this study, mostly due to the lack of adequate CO_2 observations within and around China, this study gives the first insight into the inter-annual variations of the terrestrial carbon sinks in China.

BGD

10, 1177–1205, 2013

Acknowledgements. This work was supported by the National Key Basic Research Development Program of China (Grant No: 2010CB950704 and 2010CB833503), National Natural Science Foundation of China (Grant No: 41201194), and the Priority Academic Development Program of Jiangsu Higher Education Institutions. The authors also wish to thank professor Wouter Peters at the Wageningen University and Research Center (WUR) in The Netherlands and Feng Deng at the University of Toronto in Canada for their valuable help.

References

Baker, D. F., Law, R. M., Gurney, K. R., Rayner, P., Peylin, P., Denning, A. S., Bousquet, P., Bruhwiler, L., Chen, Y. H., Ciais, P., Fung, I. Y., Heimann, M., John, J., Maki, T., Maksyutov, S., Masarie, K., Prather, M., Pak, B., Taguchi, S., and Zhu, Z.: TransCom 3 inversion intercomparison: Impact of transport model errors on the interannual variability of regional CO_2 fluxes, 1988–2003, Global Biogeochem. Cy., 20, GB1002, doi:10.1029/2004GB002439, 2006.

Bruhwiler, L. M. P., Michalak, A. M., and Tans, P. P.: Spatial and temporal resolution of carbon flux estimates for 1983–2002, Biogeosciences, 8, 1309–1331, doi:10.5194/bg-8-1309-2011, 2011.

Buitenhuis, E., Le Quéré, C., Aumont, O., Beaugrand, G., Bunker, A., Hirst, A., Ikeda, T., O'Brien, T., Piontkovski, S., and Straile, D.: Biogeochemical fluxes through mesozooplankton, Global Biogeochem. Cy., 20, GB2003, doi:10.1029/2005GB002511, 2006.

Cao, M. K., Prince, S. D., Li, K. R., Tao, B., Small, J., and Shao, X. M.: Response of terrestrial carbon uptake to climate interannual variability in China, Glob. Change Biol., 9, 536–546, 2003.

Chen, J. M., Liu, J., Cihlar, J., and Goulden, M. L.: Daily canopy photosynthesis model through temporal and spatial scaling for remote sensing applications, Ecol. Model., 124, 99–119, 1999.

Ciais P., Peylin, P., and Bousquet P.: Regional biosphere carbon fluxes as inferred from atmospheric CO_2 measurements, Ecol. Appl., 10, 1574–1589, 2000.

Deng, F. and Chen, J. M.: Recent global CO_2 flux inferred from atmospheric CO_2 observations and its regional analyses, Biogeosciences, 8, 3263–3281, doi:10.5194/bg-8-3263-2011, 2011.

BGD

10, 1177–1205, 2013

Nested Inversion for carbon sinks in China

F. Jiang et al.

Deng, F., Chen, J. M., Yuen, C. W., Ishizawa, M., Mo, G., Higuchi, K., Chan, D., Chen, B., and Maksyutov, S.: Global monthly CO_2 flux inversion with focus over North America, Tellus B, 59, 179–190, 2007.

Denning, A. S., Holzer, M., Gurney, K. R., Heimann, M., Law, R. M., Rayner, P. J., Fung, I. Y., Fan, S. M., Taguchi, S., Friedlingstein, P., Balkanski, Y., Taylor, J., Maiss, M., and Levin, L.: Three-dimensional transport and concentration of SF6 – a model intercomparison study (TransCom 2), Tellus B, 52, 266–297, 1999.

Dentener, F., van Weele, M., Krol, M., Houweling, S., and van Velthoven, P.: Trends and interannual variability of methane emissions derived from 1979–1993 global CTM simulations, Atmos. Chem. Phys., 3, 73–88, doi:10.5194/acp-3-73-2003, 2003.

Enting, I. G., Trudinger, C. M., and Francey, R. J.: A synthesis inversion of the concentration and ^{13}C of atmospheric CO_2, Tellus B, 47, 35–52, 1995.

Fang, J. Y., Guo, Z. D., Piao, S. L., and Chen, A. P.:. Terrestrial vegetation carbon sinks in China, 1981–2000, Sci. China Se. D, 50, 1341–1350, 2007 (in Chinese).

Gerbig, C., Lin, J. C., Wofsy, S. C., Daube, B. C., Andrews, A. E., Stephens, B. B., Bakwin, P. S., and Grainger, C. A.: Toward constraining regional-scale fluxes of CO_2 with atmospheric observations over a continent: 1. Observed spatial variability from airborne platforms, J. Geophys. Res., 108, 4756, doi:10.1029/2002JD003018, 2003.

Granier, C., Petron, G., Muller, J. F., and Brasseur, G.: The impact of natural and anthropogenic hydrocarbons on the tropospheric budget of carbon monoxide, Atmos. Environ., 34, 5255–5270, 2000.

Guenther, A.: The contribution of reactive carbon emissions from vegetation to the carbon balance of terrestrial ecosystems, Chemosphere, 49, 837–844, 2002.

Gurney, K. R., Law, R. M., Denning, A. S., Rayner, P. J., Baker, D., Bousquet, P., Bruhwiler, L., Chen, Y. H., Ciais, P., Fan, S., Fung, I. Y., Gloor, M., Heimann, M., Higuchi, K., John, J., Maki, T., Maksyutov, S., Masarie, K., Peylin, P., Prather, M., Pak, B. C., Randerson, J., Sarmiento, J., Taguchi, S., Takahashi, T., and Yuen, C. W.: Towards robust regional estimates of CO_2 sources and sinkes using atmospheric models, Nature, 415, 626–630, 2002.

Gurney, K. R., Law, R. M., Denning, A. S., Rayner, P. J., Baker, D., Bousquet, P., Bruhwiler, L., Chen, Y. H., Ciais, P., Fan, S. M., Fung, I. Y., Gloor, M., Heimann, M., Higuchi, K., John, J., Kowalczyk, E., Maki, T., Maksyutov, S., Peylin, P., Prather, M., Pak, B. C., Sarmiento, J., Taguchi, S., Takahashi, T., and Yuen, C. W.: TransCom 3 CO_2 inversion intercomparison: 1.

BGD
10, 1177–1205, 2013

Annual mean control results and sensitivity to transport and prior flux information, Tellus B, 55, 555–579, 2003.
Gurney, K. R., Law, R. M., Denning, A. S., Rayner, P. J., Pak, B. C., Baker, D., Bousquet, P., Bruhwiler, L., Chen, Y. H., Ciais, P., Fung, I. Y., Heimann, M., John, J., Maki, T., Maksyutov, S., Peylin, P., Prather, M., and Taguchi, S.: Transcom 3 inversion intercomparison: model mean results for the estimation of seasonal carbon sources and sinks, Global Biogeochem. Cy., 18, GB1010, doi:10.1029/2003GB002111, 2004.
Gurney, K. R., Castillo, K., Li, B., and Zhang, X.: A positive carbon feedback to ENSO and volcanic aerosols in the tropical terrestrial biosphere, Global Biogeochem. Cy., 26, GB1029, doi:10.1029/2011GB004129, 2012.
Houweling, S., Dentener, F., and Lelieveld, J.: The impact of nonmethane hydrocarbon compounds on tropospheric photochemistry, J. Geophys. Res., 103, 10637–10696, 1998.
Intergovernmental Panel on Climate Change (IPCC), I.S.A.: The Physical Science Basis of Climate Change: Changes in Atmospheric Constituents and in Radiative Forcing, Cambridge University Press, NewYork, 2007.
Jiang, F., Liu, Q., Huang, X. X., Wang, T. J., Zhuang, B. L., and Xie, M.: Regional modeling of secondary organic aerosol over China by using WRF/Chem, J. Aerosol Sci., 43, 57–73, 2012.
Ju, W. M., Chen, J. M., Black T. A., Barr A. G., Liu, J., and Chen, B. Z.: Modelling multi-year coupled carbon and water fluxes in a boreal aspen forest, Agr. Forest Meteorol., 140, 136–151, 2006.
Krol, M., Houweling, S., Bregman, B., van den Broek, M., Segers, A., van Velthoven, P., Peters, W., Dentener, F., and Bergamaschi, P.: The two-way nested global chemistry-transport zoom model TM5: algorithm and applications, Atmos. Chem. Phys., 5, 417–432, doi:10.5194/acp-5-417-2005, 2005.
Krol, M. C., Meirink, J. F., Bergamaschi, P., Mak, J. E., Lowe, D., Jöckel, P., Houweling, S., and Röckmann, T.: What can ^{14}CO measurements tell us about OH?, Atmos. Chem. Phys., 8, 5033–5044, doi:10.5194/acp-8-5033-2008, 2008.
Law, R. M., Chen, Y. H., and Gurney, K. R.: TransCom 3 CO_2 inversion intercomparison: 2. Sensitivity of annual mean results to data choices, Tellus B, 55, 580–595, 2003.
Le Quéré, C., Raupach, M. R., Canadell, J. G., Marland, G., Bopp, L., Ciais, P., Conway, T. J., Doney, S. C., Feely, R., Foster, P., Friedlingstein, P., Gurney, K., Houghton, R. A., House, J. I., Huntingford, C., Levy, P. E., Lomas, M. R., Majkut, J., Metzl, N., Ometto, J. P., Peters, G. P.,

BGD
10, 1177–1205, 2013

Nested Inversion for carbon sinks in China

F. Jiang et al.

Prentice, I. C., Randerson, J. T., Running, S. W., Sarmiento, J. L., Schuster, U., Sitch, S., Takahashi, T., Viovy, N., van der Werf, G. R., and Woodward, F. I.: Trends in the sources and sinks of carbon dioxide, Nat. Geosci., 2, 831–836, doi:10.1038/ngeo689, 2009.

Meirink, J. F., Bergamaschi, P., Frankenberg, C., d'Amelio, M. T. S., Dlugokencky, E. J., Gatti, L. V., Houweling, S., Miller, J. B., Rockmann, T., Villani, M. G., and Krol, M. C.: Fourdimensional variational data assimilation for inverse modelling of atmospheric methane emissions: analysis of SCIAMACHY observations, J. Geophys. Res., 113, D17301, doi:10.1029/2007JD009740, 2008.

Michalak, A. M., Hirsch, A., Bruhwiler, L., Gurney, K. R., Peters, W., and Tans, P. P.: Maximum likelihood estimation of covariance parameters for Bayesian atmospheric trace gas surface flux inversions, J. Geophys. Res., 110, D24107, doi:10.1029/2005JD005970, 5 2005.

Naik, V., Delire, C., and Wuebbles, D. J.: Sensitivity of global biogenic isoprenoid emissions to climate variability and atmospheric CO_2, J. Geophys. Res., 109, D06301, doi:10.1029/2003JD004236, 2004.

NASA Land Processes Distributed Active Archive Center (LP DAAC): ASTER L1B, USGS/Earth Resources Observation and Science (EROS) Center, Sioux Falls, South Dakota, 2001.

Pan, Y., Birdsey, R. A., Fang, J., Houghton, R., Kauppi, P. E., Kurz, W. A., Phillips, O. L., Shvidenko, A., Lewis, S. L., Canadell, J. G., Ciais, P., Jackson, R. B., Pacala, S., McGuire, A. D., Piao, S., Rautiainen, A., Sitch, S., and Hayes, D.: A large and persistent carbon sink in the world's forests, Science, 333, 988–993, doi:10.1126/science.1201609, 2011.

Peters, W., Krol, M., Dentener, F., Thompson, A. M., and Lelieveld, J.: Chemistry-transport modeling of the satellite observed distribution of tropical troposheric ozone, Atmos. Chem. Phys., 2, 103–120, doi:10.5194/acp-2-103-2002, 2002.

Peters, W., Miller, J. B., Whitaker, J., Denning, A. S., Hirsch, A., Krol, M. C., Zupanski, D., Bruhwiler, L., and Tans, P. P.: An ensemble data assimilation system to estimate CO_2 surface fluxes from atmospheric trace gas observations, J. Geophys. Res., 110, D24304, doi:10.1029/2005JD006157, 2005

Peters, W., Jacobson, A. R., Sweeney, C., Andrews, A. E., Conway, T. J., Masarie, K., Miller, J. B., Bruhwiler, L. M. P., Pétron, G., Hirsch, A. I., Worthy, D. E. J., van der Werf, G. R., Randerson, J. T., Wennberg, P. O., Krol, M. C., and Tans, P. P.: An atmospheric perspective on North American carbon dioxide exchange: CarbonTracker, P. Natl. Acad. Sci. USA, 104, 18925–18930, 2007.

BGD
10, 1177–1205, 2013

Nested Inversion for carbon sinks in China

F. Jiang et al.

Peylin, P., Rayner, P. J., Bousquet, P., Carouge, C., Hourdin, F., Heinrich, P., Ciais, P., and AEROCARB contributors: Daily CO_2 flux estimates over Europe from continuous atmospheric measurements: 1, inverse methodology, Atmos. Chem. Phys., 5, 3173–3186, doi:10.5194/acp-5-3173-2005, 2005.
Piao, S. L., Fang, J. Y., Ciais, P., Peylin, P., Huang, Y., Sitch, S., and Wang, T.: The carbon balance of terrestrial ecosystems in China, Nature, 458, 1009–1013, doi:10.1038/nature07944, 2009.
Rayner, N. A., Parker, D. E., Horton, E. B., Folland, C. K., Alexander, L. V., Rowell, D. P., Kent, E. C., and Kaplan, A.: Global analyses of sea surface temperature, sea ice, and night marine air temperature since the late nineteenth century, J. Geophys. Res., 108, 4407, doi:10.1029/2002JD002670, 2003.
Rayner, P. J., Enting, I. G., Francey, R. J., and Langenfelds, R.: Reconstructing the recent carbon cycle from atmospheric CO_2, ^{13}C and O_2/N_2 observations, Tellus B, 51, 213–232, 1999.
Rödenbeck, C., Houweling, S., Gloor, M., and Heimann, M.: CO_2 flux history 1982–2001 inferred from atmospheric data using a global inversion of atmospheric transport, Atmos. Chem. Phys., 3, 1919–1964, doi:10.5194/acp-3-1919-2003, 2003.
Schuh, A. E., Denning, A. S., Corbin, K. D., Baker, I. T., Uliasz, M., Parazoo, N., Andrews, A. E., and Worthy, D. E. J.: A regional high-resolution carbon flux inversion of North America for 2004, Biogeosciences, 7, 1625–1644, doi:10.5194/bg-7-1625-2010, 2010.
Tian, H., Melillo, J., Lu, C. Q., Kicklighter, D., Liu, M. L., Ren, W., Xu, X. F., Chen, G. S., Zhang, C., Pan, S. F., Liu, J. Y., and Running, S.: China's terrestrial carbon balance: contributions from multiple global change factors, Global Biogeochem. Cy., 25, GB1007, doi:10.1029/2010GB003838, 2011.
van der Werf, G. R., Randerson, J. T., Giglio, L., Collatz, G. J., Mu, M., Kasibhatla, P. S., Morton, D. C., DeFries, R. S., Jin, Y., and van Leeuwen, T. T.: Global fire emissions and the contribution of deforestation, savanna, forest, agricultural, and peat fires (1997–2009), Atmos. Chem. Phys., 10, 11707–11735, doi:10.5194/acp-10-11707-2010, 2010.
Wang, B., Huang, J. Y., Yang, X. S., Zhang, B., and Liu, M. C.: Estimation of biomass, net primary production and net ecosystem production of China's forests based on the 1999–2003 National Forest Inventory, Scand. J. Forest Res., 25, 544–553, 2010.
Wang, S. Q., Chen, J. M., Ju, W. M., Feng, X., Chen, M., Chen, P., and Yu, G.: Carbon sinks and sources in China's forests during 1901–2001, J. Environ. Manage., 85, 524–537, 2007.

BGD
10, 1177–1205, 2013

Nested Inversion for carbon sinks in China

F. Jiang et al.

Zeng, N., Mariotti, A., and Wetzel, P.: Terrestrial mechanisms of interannual CO_2 variability, Global Biogeochem. Cy., 19, GB1016, doi:10.1029/2004GB002273, 2005.
Zhao, M. S. and Running, S. W.: Drought-induced reduction in global terrestrial net primary production from 2000 through 2009, Science, 329, 940, doi:10.1126/science.1192666, 2010.
Zou, X. K., Ren, G. Y., and Zhang, Q.: Droughts variations in China based on a compound index of meteorological drought (in Chinese), Clim. Environ. Res., 15, 371–378, 2010.

BGD
10, 1177–1205, 2013

Nested Inversion for carbon sinks in China

F. Jiang et al.

Table 1. Comparison of the inverted carbon fluxes in this study with previous studies during 2002–2009.

Region	Global	Land	Ocean	North America	Europe	China
This study	−5.71 ± 1.6	−3.15 ± 1.48	−2.56 ± 0.62	−0.82 ± 0.28	−0.3 ± 0.18	−0.21 ± 0.23
Deng and Chen (2011)[1]	−5.58	−3.63 ± 0.49	−1.95 ± 0.41	−0.89 ± 0.18	−0.22	
Le Quéré et al. (2009)[2]	−5.3	−3.0 ± 0.9	−2.3 ± 0.4			

[1] Mean from 2002–2007.
[2] Mean from 2000–2008.

Discussion Paper | Discussion Paper | Discussion Paper | Discussion Paper |

BGD

10, 1177–1205, 2013

Nested Inversion for carbon sinks in China

F. Jiang et al.

Table 2. Comparison of the terrestrial carbon sinks in China derived using different methods.

Reference	Method	Period	Forest	Grass	Crop	Total
This study	Inversion method	2002–2009	−0.08 ± 0.16	−0.07 ± 0.10	−0.06 ± 0.12	−0.21 ± 0.23
Carbontracker 2010	Assimilation system	2002–2009	−0.1	−0.08	−0.07	−0.25
Tian et al. (2011)[1]	Process-based model	1961–2005	−0.115	−0.045	−0.049	−0.21 ± 0.078
Piao et al. (2009)[1]	Inventory-based method	1982–1999	−0.101	−0.037	−0.033	−0.18 ± 0.073
	Process-based model	1980–2002	–	–	–	−0.17 ± 0.073
	Inversion study	1996–2005	–	–	–	0.35 ± 0.33
Pan et al. (2011)	Inventory-based method	2000–2007	−0.115	–	–	–

[1] The carbon sinks of shrub land have been distributed to forest, grass and crop land according to the fractions of 36.8 %, 38.8 %, and 11.7 %, respectively, since the shrub land in this study are included in the forest, grass and crop regions.

BGD
10, 1177–1205, 2013

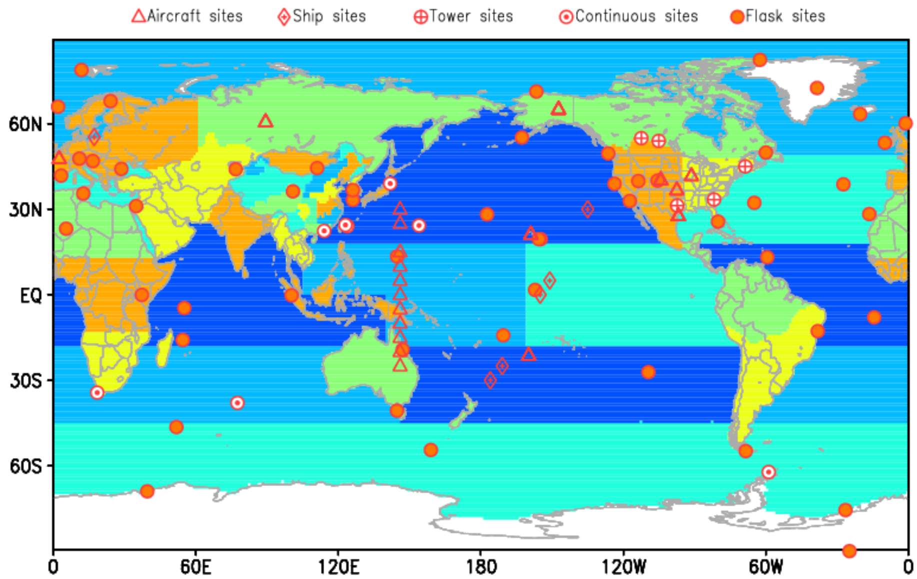

Fig. 1. An inversion scheme: 21 regions in Asia (13 regions in China) and 22 regions for the rest of the globe. Locations of 131 CO_2 observational sites are also indicated, including 54 flask sites, 8 continuous sites, 5 tower sites, 6 ship sites, 58 aircraft sites.

BGD
10, 1177–1205, 2013

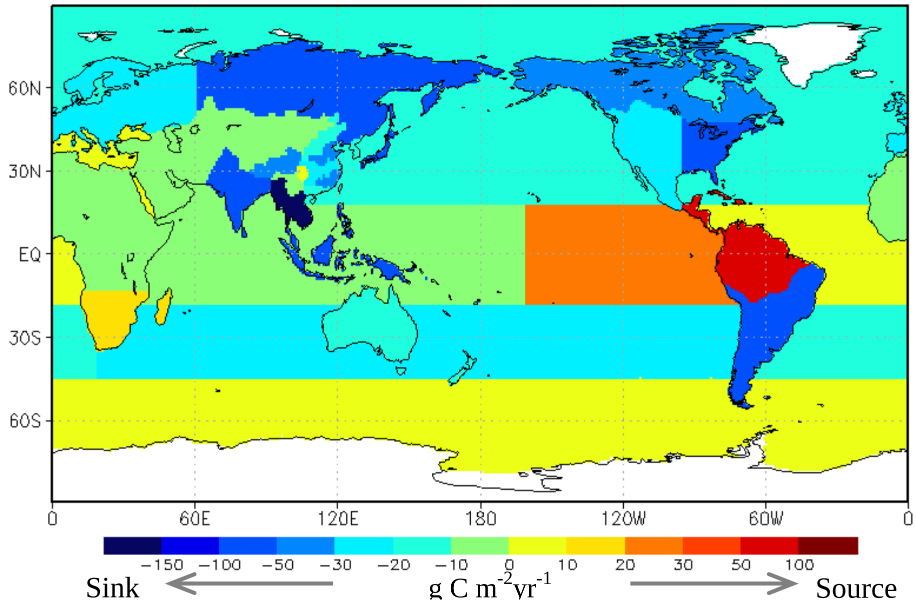

Fig. 2. Inverted mean distribution of terrestrial and ocean carbon fluxes (2002–2009).

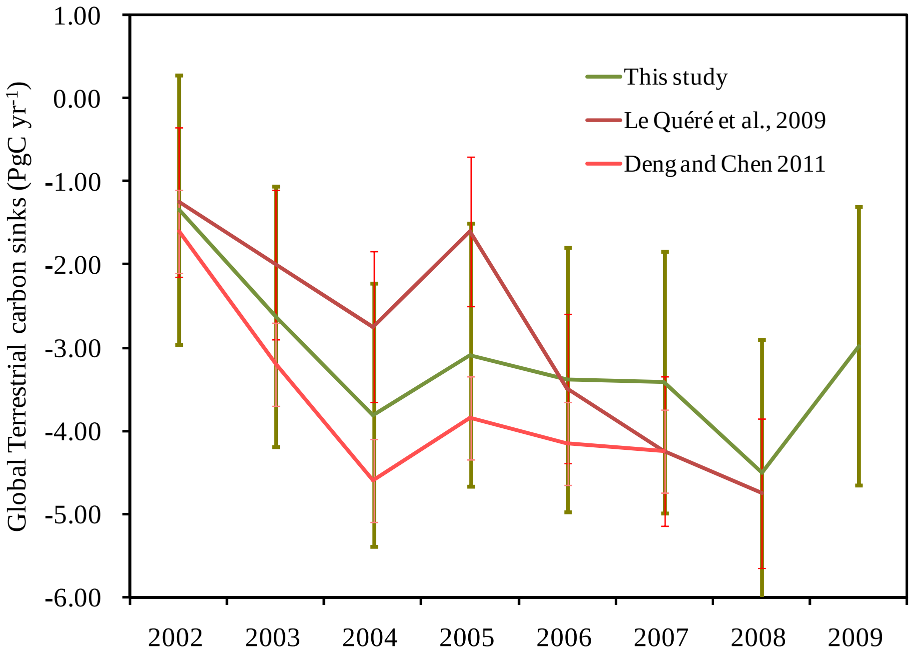

Fig. 3. Interannual variation of global terrestrial ecosystem carbon sinks (2002–2009).

BGD
10, 1177–1205, 2013

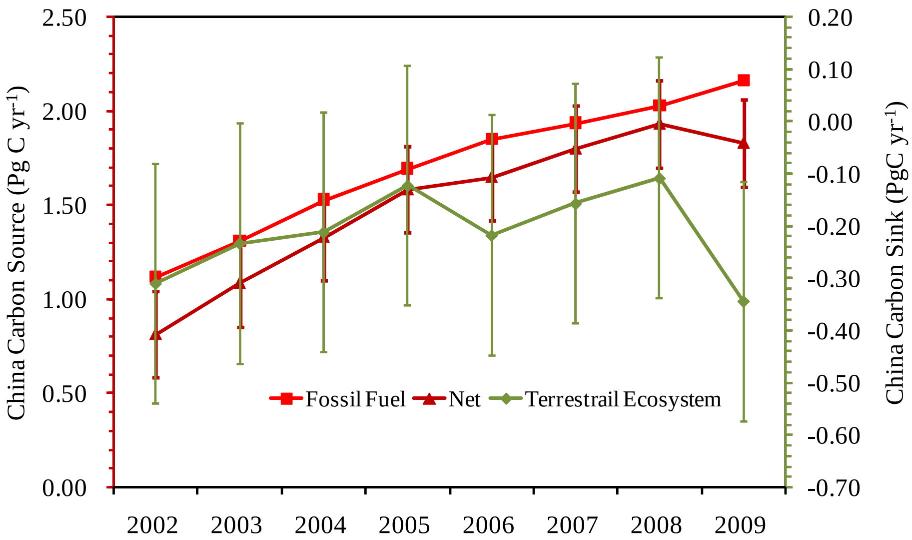

Fig. 4. Interannual variation of the terrestrial ecosystem carbon sinks, fossil fuel carbon emissions, and net carbon fluxes in China (2002–2009).

BGD
10, 1177–1205, 2013

Nested Inversion for carbon sinks in China

F. Jiang et al.

Title Page
Abstract Introduction
Conclusions References
Tables Figures
◂◂ ▸▸
◂ ▸
Back Close
Full Screen / Esc
Printer-friendly Version
Interactive Discussion

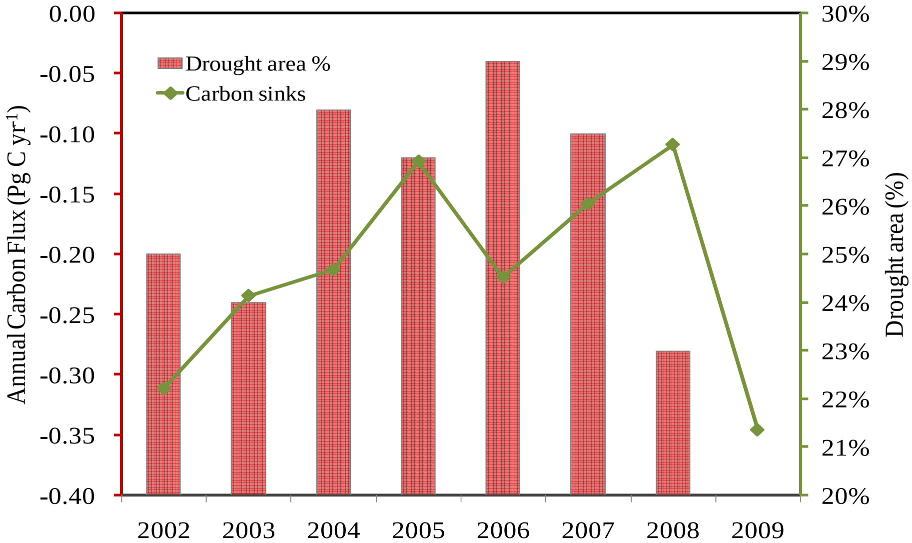

Fig. 5. Relationship between terrestrial carbon sinks and drought area in China.

BGD
10, 1177–1205, 2013

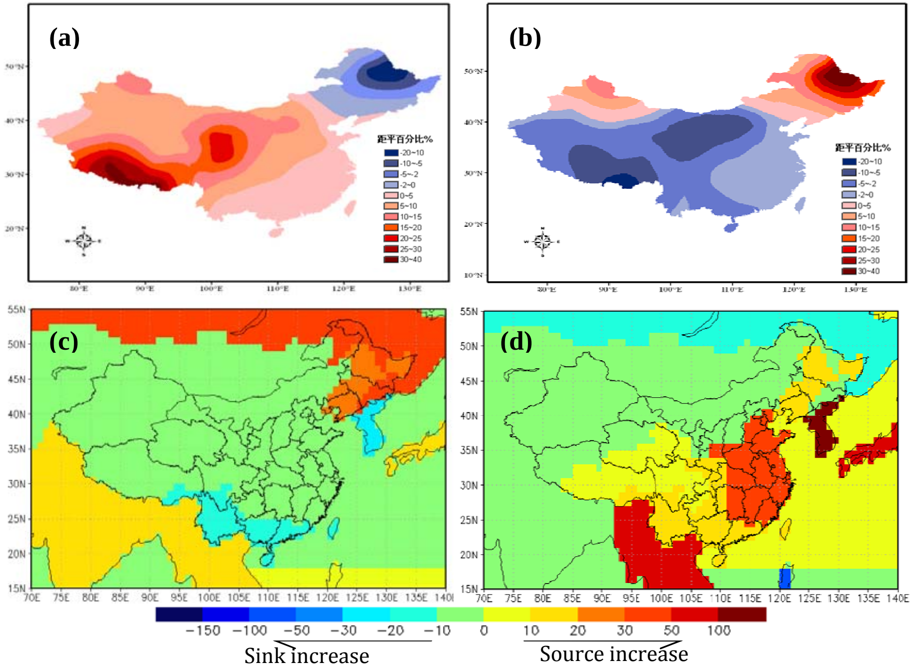

Fig. 6. Anomaly of the terrestrial carbon sinks and temperature in China. **(a, b)** Anomaly of the temperature in 2006 and 2008, respectively; **(c, d)** anomaly of the terrestrial carbon sinks in 2006 and 2008, respectively.

BGD
10, 1177–1205, 2013

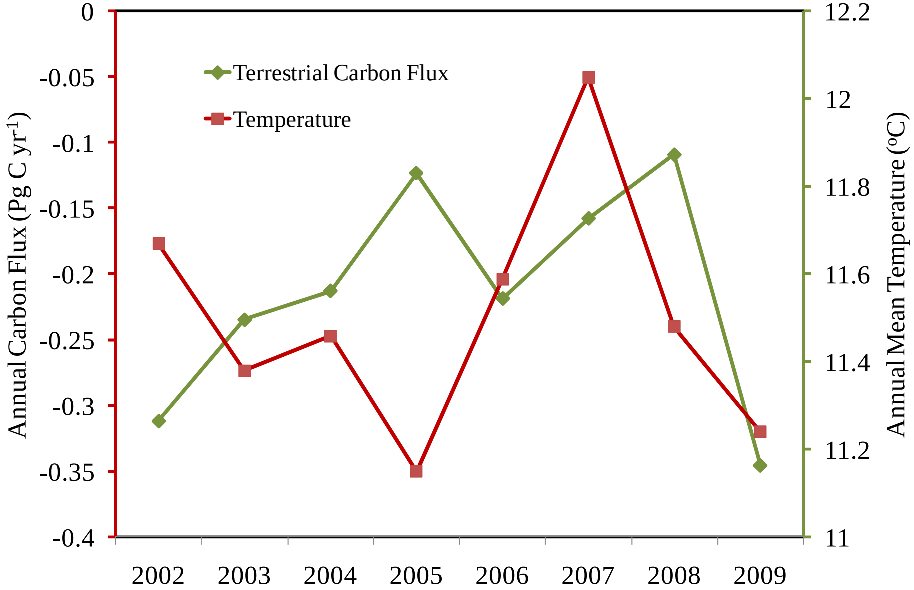

Fig. 7. Inter-annual variations of the temperature and the terrestrial carbon sink in China.

BGD
10, 1177–1205, 2013

Nested Inversion for carbon sinks in China

F. Jiang et al.